Microbiology (2005), **151**, 3817–3832 DOI 10.1099/mic.0.28165-0

Biofilm-control strategies based on enzymic disruption of the extracellular polymeric substance matrix – a modelling study

Joao B. Xavier,[1,2] Cristian Picioreanu,[2] Suriani Abdul Rani,[1] Mark C. M. van Loosdrecht[2] and Philip S. Stewart[1]

[1]Center for Biofilm Engineering and Department of Chemical and Biological Engineering, Montana State University-Bozeman, Bozeman, MT 59717-3980, USA

[2]Department of Biotechnology, Delft University of Technology, Julianalaan 67, 2628 BC Delft, The Netherlands

Correspondence
Joao B. Xavier
J.Xavier@tnw.tudelft.nl

Received 29 April 2005
Revised 29 July 2005
Accepted 21 September 2005

A kinetic model is proposed to assess the feasibility of strategies for the removal of biofilms by using substances that induce detachment by affecting the cohesiveness of the matrix of extracellular polymeric substances (EPSs). The model uses a two-state description of the EPS (natural EPS and compromised EPS) to provide a unified representation of diverse mechanisms of action of detachment-promoting agents (DPAs), which include enzymes that degrade the EPS and other agents described in the literature. A biofilm-cohesiveness factor describes local increases in detachment rates resultant from losses in cohesive strength. The kinetic model was implemented in an individual-based biofilm-modelling framework, including detachment rates dependent on local cohesiveness. The efficacy of treatments with DPAs was assessed by three-dimensional model simulations. Changes in treatment efficacy were evaluated quantitatively by using a Thiele modulus, which quantifies the relationship between diffusion of the DPA through the biofilm matrix and DPA decay rate, and a Damköhler number relating the rate of EPS reaction with a DPA and the rate of EPS production by the micro-organisms in the biofilm. This study demonstrates the feasibility and limits of implementing biofilm-control strategies based on attacking the EPS.

INTRODUCTION

Biofilms forming on the surface of indwelling medical devices by organisms such as *Staphylococcus epidermidis* and *Staphylococcus aureus* constitute a leading cause of infections (Huebner & Goldmann, 1999). In industrial settings, unwanted biofilms are responsible for the fouling of cooling-water towers, water pipelines, membrane units or food-processing plants (Jass & Walker, 2000). Several strategies to remove unwanted biofilms exist that may be applied to a particular system, depending on its characteristics (Stewart *et al.*, 2000). These include (i) mechanical cleaning, (ii) the use of antimicrobial agents, (iii) stopping biofilm growth by removing essential nutrients, (iv) inhibiting microbial attachment to a surface and (v) promoting biomass detachment. Mechanical cleaning and antimicrobial agents are the most-used methods. Mechanical cleaning can be costly, as it typically involves equipment down time or a significant labour expenditure. It may also not be applicable due to inaccessibility of the fouled surface. Still, toothbrushing remains the main method of removing dental plaque. Using biocides and disinfectants, in turn, may be ineffective due to the reduced susceptibility of micro-organisms in biofilms to antimicrobial agents [see Stewart *et al.* (2000) for a list of references]. Also, this strategy is insufficient when a clean surface, rather than one covered by an inactive biofilm, is required. Recent studies concerning induced detachment by depriving the biofilm of essential nutrients reveal the potential of this attractive strategy (Thormann *et al.*, 2005), which, however, will not be applicable to cases where controlling the nutrients in the medium is not possible.

Promoting detachment is the least investigated of the possible strategies to remove unwanted biofilms (Stewart *et al.*, 2000). The use of substances to induce biofilm removal directly by destroying the physical integrity of the biofilm matrix would be an attractive alternative for both medical and industrial applications where complete biofilm removal is essential. In industrial applications, this approach would also have the advantage of reducing reliance on inherently toxic antimicrobial agents, whose continued use is fundamentally at odds with the trend towards increasingly restrictive environmental regulations (Chen & Stewart, 2000).

Biofilms are primarily composed of bacteria, extracellular polymeric substances (EPSs) of microbial origin and other

Abbreviations: DPA, detachment-promoting agent; EPS, extracellular polymeric substance; IbM, individual-based modelling.

particulate substances. EPSs constitute a matrix embedding bacterial cells and almost certainly have essential roles in defining the cohesiveness and other physical properties of these attached microbial communities (Wingender *et al.*, 1999). Biofilm EPSs are typically composed of diverse substances, including polysaccharides, proteins, nucleic acids, lipids and humic substances (e.g. Nielsen *et al.*, 1996; Tsuneda *et al.*, 2003). Substantial evidence exists supporting the role of polysaccharides in the cohesiveness of the EPS matrix (e.g. Boyd & Chakrabarty, 1995; Hughes *et al.*, 1998). Multivalent cations such as calcium and magnesium also probably play a role in the cohesiveness of microbial aggregates, as evaluated from the study of anaerobic-sludge granules (Grotenhuis *et al.*, 1991), activated-sludge flocs (Higgins & Novak, 1997) and biofilms (Chen & Stewart, 2002), by bridging negatively charged sites on extracellular polymers to create stable intermolecular and cell–EPS connections (Mayer *et al.*, 1999).

Methods for promoting biofilm detachment by using chemical agents aimed at attacking the EPS have been investigated, so far with mixed results (Chen & Stewart, 2000). Table 1 lists several substances reported in the literature to affect the cohesiveness of EPS of bacterial origin. These substances, being enzymes, chelating agents or other agents, may reduce EPS cohesiveness through a variety of mechanisms. In the present article, all such substances that affect EPS cohesiveness and may potentially be used to promote biofilm detachment will generally be termed detachment-promoting agents (DPAs). Several enzymes have been observed to induce detachment by acting on the EPS matrix, by depolymerizing either polysaccharides (Allison *et al.*, 1998; Boyd & Chakrabarty, 1994; Chen & Stewart, 2000; Itoh *et al.*, 2005; Kaplan *et al.*, 2004; Mayer *et al.*, 1999) or extracellular DNA (Whitchurch *et al.*, 2002). Chemicals that alter the ionic strength and composition of the liquid medium and affect electrostatic interactions involved in the cohesiveness of the EPS matrix, such as salts or chelating agents (Chen & Stewart, 2000; Mayer *et al.*, 1999), may also be used as DPAs.

Fig. 1 shows results from an experiment illustrating the use of chemical substances that affect biofilm cohesiveness to cause biofilm detachment. In this experiment, an *S. epidermidis* biofilm was cultivated in a capillary biofilm reactor for 24 h as described previously (Abdul Rani *et al.*, 2005). The growth medium was then changed to a solution of 0·1 g NaOH l^{-1}. The experiment was carried out without changing the flow velocity. Biofilm structures were static prior to the introduction of NaOH. Within 1 min of the introduction of dilute NaOH, biofilm cell clusters begin to deform in the direction of flow. This suggests that the chemical treatment weakened the mechanical properties of the biofilm. The reduction in biofilm cohesiveness resulted in the detachment of biofilm cell clusters in less than 4 min after the NaOH was added.

The feasibility of strategies for removing unwanted biofilms by using DPAs is evaluated here by using mathematical modelling. A generic methodology for accessing the effectiveness of a DPA treatment based on computer simulations is proposed. Parameters concerning biofilm cohesiveness and DPA action may be customized. The mathematical model provides a three-dimensional (3D) description of biofilm dynamics based on mass conservation of the reactions involved and uses individual-based modelling (IbM; Kreft & Wimpenny, 2001), implemented in a generic software framework introduced recently (Xavier *et al.*, 2005a).

IbM was previously applied to study biofilm-structure dynamics in the presence of erosion forces in monospecies biofilms (Xavier *et al.*, 2004, 2005b), EPS production (Kreft & Wimpenny, 2001; Xavier *et al.*, 2005a, b) and multispecies biofilms (Picioreanu *et al.*, 2004; Xavier *et al.*, 2005a). Previous studies using other 2D- or 3D-modelling approaches addressed the effect of detachment caused by mechanical shear (Hermanowicz, 2001; Picioreanu *et al.*, 2001), biomass decay (Pizarro *et al.*, 2001), detachment induced by a chemical produced by the biofilm (Hunt *et al.*, 2003) and starvation (Hunt *et al.*, 2004). The present study is the first application of a multidimensional biofilm model for the evaluation of strategies for the removal of unwanted biofilms by treatment with chemical substances.

MODEL DESCRIPTION

The biofilm model used here is an extension of the framework reported previously (Xavier *et al.*, 2005a, b). Only a brief introduction of the essential model elements and description of the extensions implemented will be presented here.

Biofilm system. As in other biofilm models (e.g. Wanner & Gujer, 1986), the dynamics of two types of components are followed here. First, the soluble matter comprises any dissolved substance, such as substrates, products or DPA. Second, the particulate matter consists of solid matter, such as microbial cells and EPS. The computational volume used for the simulations represents a typical biofilm system composed of a biofilm (solid) phase and a liquid phase. Fig. 2 is a schematic representation of the system phases and geometry.

Dynamics of soluble components. Soluble matter exists both in the liquid and biofilm phases. The liquid phase is located above the biofilm and is, in turn, composed of a bulk liquid compartment and a concentration-boundary layer. The bulk liquid is assumed to be completely mixed, where solute concentrations are homogeneous and constant in time. The solute species diffuse to or from the biofilm through the concentration-boundary layer. In the biofilm phase, dynamics of solute species are governed by diffusion and reaction, as described by

$$\frac{\partial C_S}{\partial t} = \frac{\partial}{\partial x}\left(D_S \frac{\partial C_S}{\partial x}\right) + \frac{\partial}{\partial y}\left(D_S \frac{\partial C_S}{\partial y}\right) + \frac{\partial}{\partial z}\left(D_S \frac{\partial C_S}{\partial z}\right) + r_S \quad [\mathrm{M}_S\ \mathrm{L}^{-3}\ \mathrm{T}^{-1}] \quad (1)$$

here written for a growth-limiting substrate *S*. In equation (1), C_S is the substrate concentration, D_S is the diffusivity and r_S the net reaction rate. Two solute species – a growth-limiting substrate (*S*) and a soluble DPA – are considered in the present model. The two boundary conditions for each diffusion/reaction equation of type (1) are

Table 1. Candidate substances found in the literature to be used as biofilm DPAs

Agent	Origin	Substrate	Notes/action	Reference
Enzymes				
Crude cellulase preparation	*Trichoderma viride* (Maxazyme CL2000)	Dephosphorylated and partially derhamnosylated EPS of *Lactococcus lactis* subsp. *cremoris* B40	EPS was incubated with various commercial enzyme preparations and analysed for degradation In crude enzyme-preparation tests, one enzyme acted very specifically	van Casteren *et al.* (1998)
Polysaccharide depolymerase	Bacteriophage	*Enterobacter agglomerans* GFP in monospecies biofilms and in dual-species biofilms with *Klebsiella pneumoniae* G1	Phage glycanases are very specific. Action of enzyme was observed when added to the phage-susceptible monospecies biofilm, leading to substantial biofilm degradation (Hughes *et al.*, 1998) A 60 min treatment with a polysaccharase caused a 20 % reduction in dual-species biofilm adhesion (Skillman *et al.*, 1999)	
Alginate lyase	*Pseudomonas aeruginosa*	*Pseudomonas aeruginosa* alginate	Strains of *P. aeruginosa* overproducing alginate lyase detached at a higher rate than wild-type However, other studies showed that addition of alginate lyase to established *P. aeruginosa* biofilm caused no observable detachment (Christensen *et al.*, 2001)	Boyd & Chakrabarty (1994)
Disaggregatase enzyme	*Methanosarcina mazei*	*Methanosarcina mazei* heteropolysaccharide capsule mediating cell aggregation	Conditions that are generally unfavourable for growth are associated with disaggregatase activity	Xun *et al.* (1990)
Esterases with wide specificity	Wide range of bacteria	Acyl residues from bacterial polymers as well as other esters	Acetyl residues from intracellular carboxylesterase (EC 3.1.1.1) isolated from *Arthrobacter viscosus* removed acetyl residues from xanthan, alginate, glucose pentaacetate, cellobiose octaacetate, exopolysaccharide produced by *A. viscosus*, deacetylated *p*-nitrophenyl propionate, naphthyl acetate, isopropenyl acetate and triacetin (Cui *et al.*, 1999) Esterases could alter the physical properties of a biofilm structure	Sutherland (2001)
Dispersin B (or DspB)	*Actinobacillus actinomycetemcomitans*	Poly-β-1,6-GlcNAc implicated as an adhesion factor for biofilms of several bacterial species	Causes detachment of cells from *A. actinomycetemcomitans* biofilms and disaggregation of clumps of *A. actinomycetemcomitans* in solution (Kaplan *et al.*, 2003) Treatment of *S. epidermidis* biofilms with dispersin B causes dissolution of the EPS matrix and detachment of biofilm cells from the surface (Kaplan *et al.*, 2004) Disrupts biofilm formation by *E. coli*, *S. epidermidis*, *Yersina pestis* and *Pseudomonas fluorescens* (Itoh *et al.*, 2005)	
DNase I	Commercial (Sigma-Aldrich)	Extracellular DNA in *Pseudomonas aeruginosa* biofilms	DNase affects the capability of *P. aeruginosa* to form biofilms when present in the initial development stages. Established biofilms were only affected to a minor degree by the presence of DNase	Whitchurch *et al.* (2002)

Table 1. cont.

Agent	Origin	Substrate	Notes/action	Reference
Mixtures of enzymes	Commercial	*S. aureus*, *S. epidermidis*, *P. fluorescens* and *P. aeruginosa* biofilms on steel and polypropylene substrata	Pectinex UltraSP (Novo Nordisk A/S, a multicomponent enzyme preparation) reduced the number of bacterial cells in biofilms on stainless steel without any significant bactericidal activity (the activity of Pectinex Ultra is mainly a degradation of extracellular polysaccharides)	Johansen *et al.* (1997)
		S. mutans, *Actinomyces viscosus* and *Fusobacterium nucleatum* biofilms on saliva-coated hydroxyapatite	Mutanase and dextranase were shown to remove oral plaque from hydroxyapatite, but were not bactericidal (Novo Nordisk A/S)	
Other agents				
Chelating agents		*Pseudomonas aeruginosa* biofilm or alginate from from mucoid *P. aeruginosa*	EGTA, a calcium-specific chelating agent, effected the immediate and substantial detachment of a *P. aeruginosa* biofilm without affecting microbial activity (Turakhia *et al.*, 1983)	
			EDTA and other chelating agents produced major reductions in alginate gel strength (Gordon *et al.*, 1991)	
			EDTA and Dequest 2006 reduced viscosity of a suspension of two-species biofilms of *P. aeruginosa* and *Klebsiella pneumoniae* (Chen & Stewart, 2000)	
NaCl, $CaCl_2$ or $MgCl_2$		*Pseudomonas aeruginosa* biofilm or alginate from from mucoid *P. aeruginosa*	Tests using several slime dispersants, including sodium salts and chelating agents, determined that alginate gel strength is reduced by sodium salts, albeit to a lesser extent than that observed by using chelating agents (Gordon *et al.*, 1991)	
			Treatment of intact biofilm with NaCl, $CaCl_2$ or $MgCl_2$ resulted in the rapid detachment of a significant percentage of the total biofilm protein (Chen & Stewart, 2000)	
			Increasing the ionic strength of the medium presumably screens out cross-linking electrostatic interactions, diminishing biofilm cohesiveness (Chen & Stewart, 2002)	
Surfactants		Two-species biofilms of *P. aeruginosa* and *Klebsiella pneumoniae*	Reduction in total biofilm protein observed, possibly resulting from a disruption of hydrophobic interactions involved in cross-linking the biofilm matrix (Chen & Stewart, 2000)	
Urea		Two-species biofilms of *P. aeruginosa* and *Klebsiella pneumoniae*	Treatment with urea caused a 46 % reduction in the apparent viscosity of the biofilm suspension, suggesting a role for hydrogen bonding in cross-linking the biofilm (Chen & Stewart, 2000)	

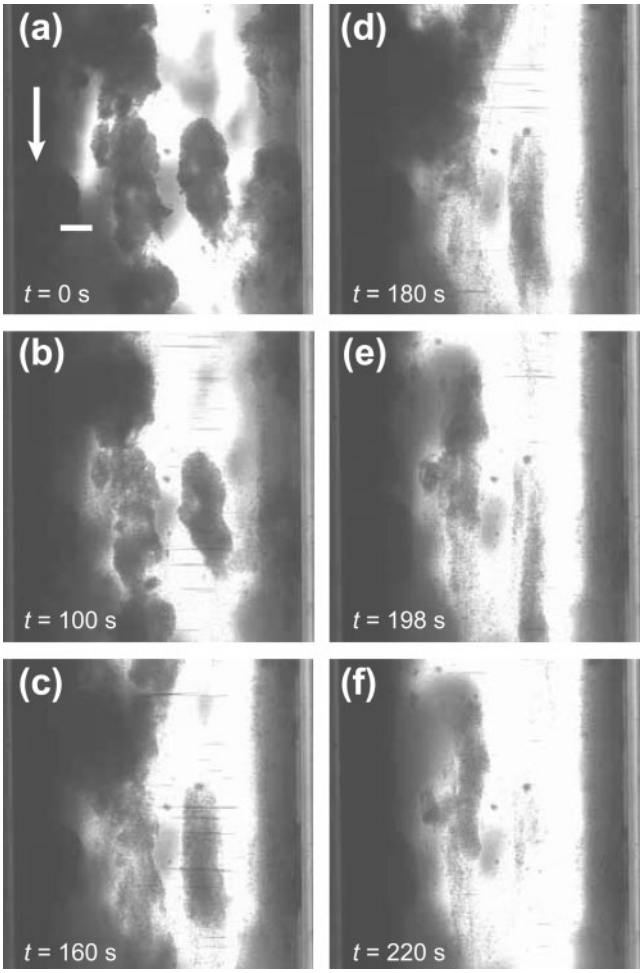

Fig. 1. Transmission-mode scanning laser microscopy of *S. epidermidis* biofilms grown for 24 h in a glass capillary tube. The image sequence, from (a) to (f), shows the deformation of a biofilm cluster and its consequent detachment after changing the influent medium to a solution with 0·1 g NaOH l^{-1}. The time shown in each panel is the time elapsed from the change in medium to the NaOH solution. The flow velocity was kept constant during the experiment [flow direction is from top to bottom, as represented by the arrow in (a)]. Bar, 10 μm. A video of the experiment is also available at http://www.biofilms.bt.tudelft.nl/biofilmControl/index.html.

(i) a specified concentration at the interface between boundary layer and bulk liquid and (ii) no-flux condition ($\partial C_S/\partial x = 0$) at the substratum on which the biofilm grows.

Dynamics of particulate components

Representation. Biofilm matter (biomass or particulate components) is represented in terms of its composition in active biomass (i.e. living micro-organisms) and EPS. For simplicity, it is assumed here that particulate matter exists only in the biofilm phase and not in the liquid phase. The IbM approach is used for the spreading of the biofilm matter as described previously (Xavier *et al.*, 2005a). In the original framework, only one EPS type was allowed for each active biomass species. In this study, the framework is extended to allow EPS composition to include any number of particulate species. This extension permits implementation of two EPS states, 'cohesive' (natural EPS) and 'compromised' (EPS altered by DPA, denoted here as EPS*), with consequences that will be explained further. In IbM, biomass is represented by using spherical particles that act independently. These particles are entities with an internal state, defined in the present work in terms of their biomass composition (in active mass, EPS and EPS*), size and location in space. The size (volume, V_p) of a particle is related to its composition. Each of the biomass components, such as the active mass (M_X), the EPS mass (M_{EPS}) and the EPS* mass (M_{EPS^*}), accounts for a volume related to its specific mass (ρ):

$$V_p = \frac{M_X}{\rho_X} + \frac{M_{EPS}}{\rho_{EPS}} + \frac{M_{EPS^*}}{\rho_{EPS^*}} \quad [L^3] \tag{2}$$

The radius of a spherical particle, R_p, is determined directly from that volume by using

$$R_p = \sqrt[3]{\frac{3V_p}{4\pi}} \quad [L] \tag{3}$$

Processes. Biomass particles follow behaviour rules that mimic the behaviour of a microbial cell. They can: (i) grow by intake of nutrients; (ii) divide, creating an offspring agent; (iii) move (in continuous spatial coordinates) when pushed by neighbouring particles; and (iv) produce and excrete EPS. In addition, biomass particles can be removed from the biofilm body by any detachment mechanism. Growth of the spherical biomass particles occurs when active biomass or EPS is produced, the production of which is governed by equations (4) and (6), respectively. Moving follows the iterative procedure of the IbM, where the individuals (biomass particles) shove each other every time step to undo any overlap between neighbours generated by divisions and growth.

Kinetics. The growth rate of active biomass ($r_{X,prod}$) is governed by a Monod-type expression:

$$r_{X,prod} = \mu_{max} \frac{C_S}{C_S + K_S} C_X \quad [M_X\ L^{-3}\ T^{-1}] \tag{4}$$

where μ_{max} is the maximum specific growth rate of the micro-organisms, C_S is the concentration of the growth limiting substrate, K_S is the Monod half-saturation constant and C_X is the concentration of active biomass. The consumption rate of substrate, $r_{S,cons}$, is related to growth of active biomass through a yield coefficient Y_S, according to

$$r_{s,\,cons} = -Y_s r_{x,\,prod} \quad [M_S\ L^{-3}\ T^{-1}] \tag{5}$$

The rate of EPS production ($r_{EPS,prod}$) is assumed to be coupled to biomass growth and related to $r_{X,prod}$ by a yield coefficient Y_{EPS}, as described previously (Stewart, 1993):

$$r_{EPS,\,prod} = Y_{EPS} r_X \quad [M_{EPS}\ L^{-3}\ T^{-1}] \tag{6}$$

The model proposed here also addresses the possibility of inactivation of the DPA. An example of an inactivation process is the decay of the DPA, applicable for instance in the case where the DPA is an enzyme. For simplicity, first-order decay rate will be used to model this case:

$$r_{DPA,\,dec} = -k_{DPA,dec} C_{DPA} \quad [M_{DPA}\ L^{-3}\ T^{-1}] \tag{7}$$

Stoichiometry and rates of reactions used by the current biofilm model are presented in Table 2.

Biomass detachment. Detachment occurring from both erosion and sloughing was included following a methodology introduced previously (Xavier *et al.*, 2005b). Briefly, the detachment model uses

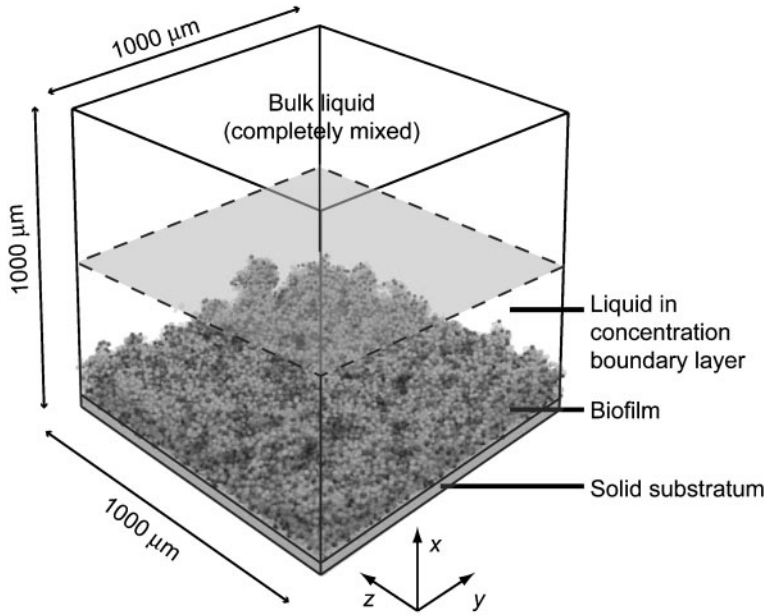

Fig. 2. Schematic representation of the system used in simulations, describing a computational volume of $1000 \times 1000 \times 1000\ \mu m^3$. The biofilm phase, comprising active biomass and EPS, develops on a planar solid substratum. The liquid phase on top of the biofilm is divided into a bulk region of constant concentration of soluble species (an infinite reservoir) and a boundary layer concentrating the whole external resistance to mass transfer of soluble species.

a detachment-speed function, F_{det}, to calculate the local biomass erosion. $F_{det}(\mathbf{x})$ is the retraction speed of the biofilm–liquid interface at a point $\mathbf{x}$ located on the biofilm–liquid interface. The speed is defined in the direction normal to the surface and expressed by

$$\frac{d\mathbf{x}}{dt} = -F_{det}(\mathbf{x})\mathbf{n}(\mathbf{x}) \quad [\mathrm{L\ T^{-1}}] \tag{8}$$

where $\mathbf{n}(\mathbf{x})$ is the vector normal to the surface at point $\mathbf{x}$. Point $\mathbf{x}$ is defined as $\mathbf{x}=(x,y,z)$, with x being the direction perpendicular to the planar substratum and y and z being the directions parallel to the substratum. The expression for F_{det} is arbitrary, as it is possible to use a function of any state variable. Sloughing occurs whenever biomass clusters become disconnected from the biofilm body.

Introducing the influence of biofilm cohesiveness in the detachment expression. Detachment occurs when external forces acting on the biofilm exceed the local biofilm cohesiveness. A biofilm cohesiveness factor, χ, is proposed here, so that the local detachment speed is inversely proportional to χ:

$$F_{det}(\mathbf{x}) \propto \frac{1}{\chi(\mathbf{x})} \tag{9}$$

In equation (9), $\chi(\mathbf{x})$ refers to the local value of the biofilm cohesiveness at location $\mathbf{x}$ on the biofilm/liquid interface.

A detachment-speed function used previously for modelling biofilm development on a planar substratum (Xavier *et al.*, 2004, 2005b) included a dependence on the square of the distance to the solid substratum, x^2, and the local biofilm density, $\rho(\mathbf{x})$, as follows:

$$F_{det}(\mathbf{x}) = \frac{k_{det}x^2}{\rho(\mathbf{x})} \quad [\mathrm{L\ T^{-1}}] \tag{10}$$

The value for the local biofilm density, $\rho(\mathbf{x})$, used in this expression is the total biomass (all types of EPS and active mass) per unit volume. It is noteworthy that this modelling framework allows for other types of detachment functions to be used, allowing the model to be customized for each particular system. The dependence on x^2 was chosen because it is used commonly in biofilm studies (Stewart, 1993; Wanner & Gujer, 1986; Xavier *et al.*, 2004, 2005b) and ensures the existence of a steady state (Stewart, 1993). The detachment-speed coefficient in equation (10), k_{det}, can be used to alter the effect of the external forces acting on the biofilm. Equation (10) may be interpreted as a balance between external forces acting on the biofilm (the product $k_{det}x^2$) and its cohesive forces, here proportional to the local biofilm density, $\rho(\mathbf{x})$:

$$\chi(\mathbf{x}) \propto \rho(\mathbf{x}) \tag{11}$$

In the present study, equation (10) will be extended to include the role of EPS In the cohesiveness of the biofilm matrix. In order to encompass

Table 2. Stoichiometry and rates of reactions defined in the model system

Columns represent the species in the system, rows represent the reactions and entries in the table represent the stoichiometric coefficients (empty entries are effectively 0). The last column shows the expressions for reaction rates of each process.

Process	Solute species		Particulate species			Rate
	Substrate (S)	Potential detachment promoter (DPA)	Active biomass (X)	EPS – cohesive state (EPS)	EPS – compromised state (EPS*)	
Growth	$-Y_S$		1	Y_{EPS}		$\mu^{\max}\frac{C_S}{C_S+K_S}C_X$
EPS decay				-1	Y_{EPS^*}	$k_{EPS,dec}\frac{C_{EPS}}{C_{EPS}+K_{EPS}}C_{DPA}$
DPA decay		-1				$k_{DPA,dec}C_{DPA}$

the generality of mechanisms for the action of DPAs, two states for EPS, the 'cohesive state' and the 'compromised state', are proposed. The cohesive state (represented by subscript *EPS*) refers to EPS in its normal state, which provides the biofilm with its natural characteristics. This is a general representation of the EPS that groups all its possible components (polysaccharides, proteins, etc.). The compromised state (represented by subscript *EPS**) refers to a denatured state of the EPS after reacting with a DPA. Consequently, two EPS concentrations are distinguished, C_{EPS} and C_{EPS^*}, as mass of EPS per biofilm volume.

The rate of EPS decomposition, $r_{EPS,dec}$, will depend on the type of the DPA used. For example, if the DPA is an enzyme, Michaelis–Menten kinetics may be used:

$$r_{EPS,dec} = -k_{EPS,dec} \frac{C_{EPS}}{C_{EPS} + K_{EPS}} C_{DPA} \quad [\mathrm{M}_{EPS}\ \mathrm{L}^{-3}\ \mathrm{T}^{-1}] \tag{12}$$

In equation (12), $k_{EPS,dec}$ is a decomposition-rate coefficient, C_{DPA} is the DPA concentration and K_{EPS} is the Michaelis–Menten (or saturation) coefficient.

Conversion of EPS into EPS* will depend on the particular composition of the biofilm EPS. The following generic expression is proposed here:

$$r_{EPS^*,prod} = -Y_{EPS^*} r_{EPS,dec} \quad [\mathrm{M}_{EPS^*}\ \mathrm{L}^{-3}\ \mathrm{T}^{-1}] \tag{13}$$

where Y_{EPS^*} is the yield of mass of EPS* produced per mass of EPS decomposed. In practice, Y_{EPS^*} will have a value of 1 for DPAs that affect matrix cohesiveness without degrading the EPS. This may be the case for chelating agents and other substances that alter electrostatic interactions (and hence biofilm cohesiveness), but that do not decrease the mass of EPS in the biofilm. As the biofilm EPS may comprise a variety of polymers, enzymes that degrade only certain polymers in the EPS will generate a value between 0 and 1 for Y_{EPS^*}. In these cases, a quantity $(1 - Y_{EPS^*})$ of soluble products from the EPS degradation would be formed. These products are assumed to have no subsequent influence on the system (i.e. are not biodegradable and do not react with any of the system's components) and therefore will not be included in the model formulation.

If we define the local fraction of EPS in its cohesive state, relative to the total EPS (cohesive and compromised states), as

$$f_{EPS} = \frac{C_{EPS}}{C_{EPS} + C_{EPS^*}} \quad [\text{dimensionless}] \tag{14}$$

then equation (10) can be extended to include the effect of the f_{EPS} on the biofilm cohesiveness, as a power–law dependency:

$$\chi(\mathbf{x}) \propto \rho(\mathbf{x}) \cdot f_{EPS}^{\gamma} \quad \text{with} \quad \gamma > 0 \tag{15}$$

This states that biofilm cohesiveness decreases with a decreasing fraction of cohesive EPS, f_{EPS}. Any order (γ) of the dependence on f_{EPS} may be used, depending on the particular case being modelled. The order γ will reflect the importance of the EPS components affected by the DPA for the biofilm cohesiveness. An expression that extends the detachment function (equation 10) is then derived from equation (15):

$$F_{det}(\mathbf{x}) = \frac{k_{det}}{(f_{EPS}(\mathbf{x}))^{\gamma}\ \rho(\mathbf{x})} x^2, \quad \text{with} \quad \gamma > 0 \quad [\mathrm{L}\ \mathrm{T}^{-1}] \tag{16}$$

and includes the dependence on f_{EPS} of the biofilm cohesiveness.

Simulations carried out. Parameters for biomass growth and EPS production obtained from the literature were used in the simulations and are listed in Table 3. The effectiveness of biofilm removal using a DPA was evaluated by the time course of the simulated reduction of active mass in the biofilm. Several scenarios were evaluated, considering various characteristics of the DPA. A set of six variables defines each particular scenario. These variables are the diffusivity of the DPA (D_{DPA}), the decay-rate coefficient of the DPA ($k_{DPA,dec}$), the concentration of DPA used in the treatment ($C_{DPA,treat}$), the decay-rate coefficient of the EPS ($k_{EPS,dec}$), the yield (Y_{EPS^*}) and the order of the EPS cohesiveness dependence on f_{EPS} (γ). The first two variables may be grouped, together with the biofilm thickness, L_f, in a dimensionless number, the Thiele modulus ϕ, defined as

$$\phi^2 = \frac{k_{DPA,dec} L_f^2}{D_{DPA}} \quad [\text{dimensionless}] \tag{17}$$

The value for L_f used in equation (17) is the maximum biofilm thickness at the time of application of the DPA treatment. This ϕ number thus relates the timescales of DPA diffusion and decay. $k_{EPS,dec}$ and $C_{DPA,treat}$ may be grouped in the dimensionless Damköhler number, defined as

$$Da = \frac{k_{EPS,dec} C_{DPA,treat}}{Y_{EPS} \mu^{\max} \rho_X} \quad [\text{dimensionless}] \tag{18}$$

This *Da* number relates the timescale of cohesive EPS decay to the timescale of EPS production by the micro-organisms. The remaining two variables from the set, Y_{EPS^*} and γ, are addressed independently. Y_{EPS^*} was varied to represent scenarios in which the EPS mass is degraded at varying degrees. The effect of parameter γ on biofilm removal was also assessed by carrying out simulations with values of γ ranging from 0·2 to 10.

Animations concerning all of the simulations analysed in the present study were also produced. These animations may be obtained in the form of digital video files from our website at http://www.biofilms.bt.tudelft.nl/biofilmControl/index.html.

RESULTS

Characterization of growth of undisturbed biofilms

The dynamics of an undisturbed biofilm (i.e. growing in the absence of any DPA) was first studied by simulating a period of 100 days growth. Four replicate simulations (U1, U2, U3 and U4) were carried out with the aims of (i) assessing reproducibility of the steady state and (ii) allowing statistically significant comparison with the results from the treatment-scenario simulations later. All simulations started from an initial state consisting of 3200 biomass particles placed randomly on the solid substratum surface. The difference between replicates is given by the initial position of biomass particles and by the sequence of random events in the shoving algorithm [see Xavier *et al.* (2004) for details]. Results of the replicate simulations showed the presence of a reproducible initial development stage in the first 10 days growth. After the occurrence of the first sloughing events at approximately $t = 12$ days, structure dynamics are no longer quantitatively reproducible, similarly to what has been reported from experiments (Lewandowski *et al.*, 2004) and other simulations (Xavier *et al.*, 2004). Fig. 3 shows results from biofilm simulation U1. Observation of the computed biofilm dynamics throughout the entire simulated period allows the conclusion that the biofilm reached a 'noisy' steady state after 20 days growth. From this time, long-term biofilm accumulation is negligible (Fig. 3a), with

Table 3. Parameters used in simulations

Parameter	Description	Value	Unit	Notes/reference
D_S	Diffusivity of substrate	$4{\cdot}2 \times 10^{-6}$	$m^2\ h^{-1}$	Rittmann *et al.* (2004)
ρ_X	Specific mass of active biomass	200	g $X\ l^{-1}$	Within the range measured by Staudt *et al.* (2004)
ρ_{EPS}	Specific mass of EPS (cohesive state)	33	g EPS l^{-1}	Six times less dense than active biomass of Horn *et al.* (2001)
ρ_{EPS^*}	Specific mass of EPS (compromised state)	33	g EPS l^{-1}	Assumed to be the same as ρ_{EPS}
μ_{max}	Maximum specific growth rate of micro-organisms	0·5	g X (g X)$^{-1}$ h^{-1}	Rittmann *et al.* (2004)
Y_{EPS}	Yield of EPS produced per biomass produced	1·4	g EPS (g X)$^{-1}$	Horn *et al.* (2001)
Y_S	Yield of oxygen consumed per biomass produced	1·63	g S (g X)$^{-1}$	Rittmann *et al.* (2004)
K_S	Half-saturation constant of substrate for biomass growth	4×10^{-3}	g $S\ l^{-1}$	Rittmann *et al.* (2004)
K_{EPS}	Half-saturation constant of EPS for EPS decay	3·3	g EPS l^{-1}	Assumed (10 % of ρ_{EPS})
Inoculation				
N_{ini}	Initial no. biomass particles	3200	–	
	Composition of initial particles:			
	Active mass	$7{\cdot}5 \times 10^{-11}$	g X	
	EPS	$1{\cdot}0 \times 10^{-10}$	g EPS	
Environmental conditions				
C_S^{bulk}	Bulk concentration of substrate	1×10^{-3}	g $S\ l^{-1}$	
k_{det}	Detachment-rate coefficient	1×10^5	g $m^{-4}\ h^{-1}$	
Numeric parameters				
$L_x \times L_y \times L_z$	Size of computational volume	$1000 \times 1000 \times 1000$	μm^3	
R_{div}	Radius of division of biomass particles	10	μm	
	No. grid nodes for solute-concentration field	$33 \times 33 \times 33$		
Variables				
$C_{DPA,treat}$	Treatment concentration of DPA	(variable)	g DPA l^{-1}	Grouped in Da (equation 18)
D_{DPA}	Diffusivity of DPA	(variable)	$m^2\ h^{-1}$	Grouped in ϕ (equation 17) and ϕ' (equation 20)
$k_{DPA,dec}$	DPA decay-rate coefficient	(variable)	g DPA (g DPA)$^{-1}$ h^{-1}	Grouped in ϕ (equation 17)
$k_{EPS,dec}$	EPS decay-rate coefficient	(variable)	g EPS (g DPA)$^{-1}$ h^{-1}	Grouped in Da (equation 18) and ϕ' (equation 20)
Y_{EPS^*}	Yield of EPS* produced per EPS consumed	(variable)	g EPS* (g EPS)$^{-1}$	
γ	Order of the EPS cohesiveness dependence on f_{EPS}	(variable)	[dimensionless]	(see equations 15 and 16)
Y_{DPA}	Yield of DPA decay for the cases when DPA is involved in a stoichiometric reaction	(variable)	g DPA (g EPS)$^{-1}$	Grouped in ϕ' (equation 20)

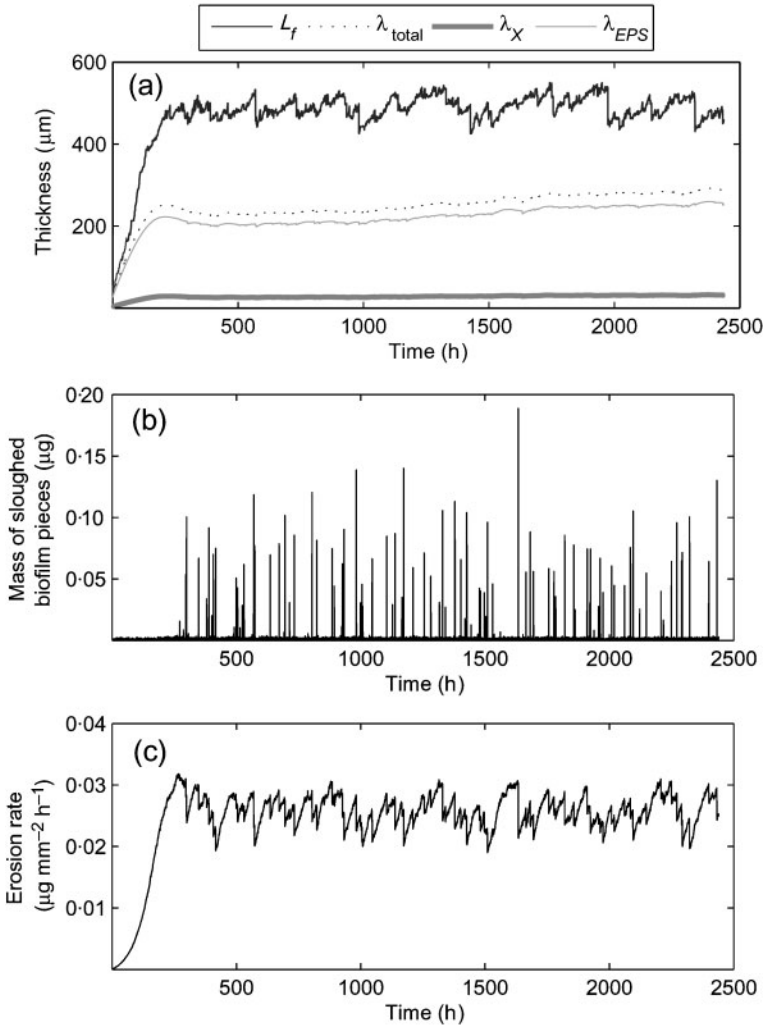

Fig. 3. Results from simulation U1 of undisturbed biofilm growth for 100 days (2400 h). (a) Time course of maximum biofilm thickness (L_f) and equivalent thickness of total biomass (λ_{total}), of active biomass (λ_X) and of EPS (λ_{EPS}) in the biofilm. Equivalent thickness of a biomass component i in the biofilm is defined by $\lambda_i = \frac{\sum_{j=1}^{N_p} M_{i,j}}{\rho_i} \cdot \frac{1}{L_y L_z}$, where $M_{i,j}$ is the mass of component i in biomass particle j. The whole biofilm contains N_p particles. (b) Sloughing events occurring in the course of biofilm development, shown as the mass of biofilm particles detached by sloughing. (c) Time course of the rate of biomass erosion from the biofilm.

time average biomass-production rate practically balancing the biomass losses by detachment (Table 4). The steady state of the undisturbed biofilm was further characterized by the occurrence of frequent sloughing events. Fig. 3(b, c) shows that erosion accounted for about 80 % of the total biomass losses, whereas sloughing accounted for only 20 %. Detachment by sloughing originated a distribution of sizes of detached particles, shown in Fig. 4, which was fitted to a normal distribution (also shown).

Simulation of treatment with a DPA

Several treatment scenarios were simulated by using different sets of parameter values. These simulations were all carried out using the same initial state, i.e. the biofilm from simulation U1 at day 60. Fig. 5 shows the results from a sample simulation, following a typical pattern observed for all simulations in which the biofilm was fully removed. The simulated conditions correspond to treatment with an enzymic DPA with the relatively low values of $\phi = 3{\cdot}6$ and $Da = 0{\cdot}71$ and at $Y_{EPS^*} = 1$ (total EPS conversion to EPS*). In this simulation, complete biofilm removal was achieved after 23·3 h DPA treatment. This case corresponds to a practical case where the DPA is an enzyme that diffuses rapidly through the biofilm (quantified by a low value of ϕ), catalysing EPS conversion to EPS* very quickly relative to the rate at which EPS is produced (quantified by the low Da value). Most removal, corresponding to 99 % of the active biomass, occurred in the relatively short period ranging from $t = 0$ to 2·7 h (as seen in Fig. 5e). During the same period, large changes in the biofilm porosity [represented in Fig. 5(f)] were also observed. Biofilm finger-like structures [observable in the 3D representation in Fig. 5(a)] were destroyed first by the action of the DPA. As a result, a more homogeneous structure was formed temporarily [as seen in Fig. 5(b)] and the porosity of the biofilm, ε, decreased until $t = 1{\cdot}4$ h. After 1·4 h, the porosity increased again ($\varepsilon \rightarrow 1$) as the biomass at the solid substratum started to detach and colonization at the substratum became sparse (Fig. 5c). Detachment of the last 1 % of the micro-organisms required a comparatively long time, corresponding to 94 % of the total treatment time. Most of the detachment occurred from enhanced erosion and not from sloughing. Erosion rates [red line in Fig. 5(g)] at early treatment time (until $t = 2{\cdot}4$ h) are well above the mean for undisturbed biofilm growth (Fig. 3c). This enhanced erosion rate is a direct consequence

Table 4. Mean biofilm properties at 'steady state' for the simulations of undisturbed development

Averaging was done between days 20 and 100.

Simulation	Thickness (μm)	Active mass (mg m^{-2})	Erosion rate (mg m^{-2} day^{-1})	Sloughing rate (mg m^{-2} day^{-1})	Total detachment rate (erosion + sloughing) (mg m^{-2} day^{-1})	Biomass-production rate (mg m^{-2} day^{-1})	Biomass accumulation (mg m^{-2} day^{-1})
U1	491·0 ± 48·3	2315 ± 320	0·0258 ± 0·0046	0·0062 ± 0·0477	0·0320 ± 0·0475	0·0325 ± 0·0024	0·0005 ± 0·0476
U2	487·5 ± 59·4	2407 ± 251	0·0256 ± 0·0058	0·0060 ± 0·0468	0·0316 ± 0·0467	0·0322 ± 0·0028	0·0006 ± 0·0467
U3	487·2 ± 47·6	2375 ± 265	0·0256 ± 0·0054	0·0061 ± 0·0456	0·0317 ± 0·0454	0·0323 ± 0·0023	0·0006 ± 0·0454
U4	488·2 ± 53·9	2373 ± 253	0·0254 ± 0·0051	0·0062 ± 0·0463	0·0316 ± 0·0461	0·0322 ± 0·0025	0·0006 ± 0·0461

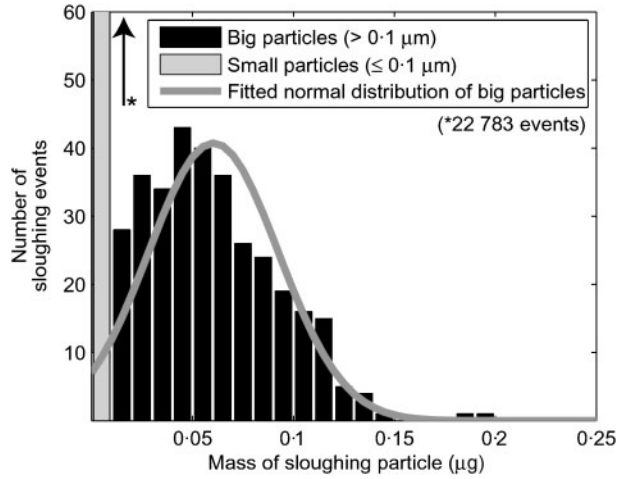

Fig. 4. Distribution of biomass particle sizes sloughed during simulation of undisturbed biofilm. Particle count corresponds to the total of the four replicate simulations carried out. Detachment events are discriminated as either big (particles > 0·01 μg, ~330 particles in total) or small (particles ≤ 0·01 μg, more than 22 000 particles in total, considered as erosion); see text for details. Also shown is the normal distribution of big particles sloughed, showing a mean ± SD value of 0·060 ± 0·032 μg.

of the higher fraction of the weak and detachable compromised EPS [see red areas in Fig. 5(b, c)] produced by DPA action. Sloughing during the treatment [blue line in Fig. 5(g)] accounted for <3% of the total detached biomass (black line). No sloughing of big biofilm sections occurred.

Treatment simulations were carried out for a range of values of ϕ and *Da*, while keeping all other parameters constant. A high value of ϕ means fast DPA decay relative to its diffusion rate (equation 17). A high value of *Da* means fast EPS degradation by DPA relative to the EPS production rate (equation 18). Therefore, a high *Da* number corresponds to high DPA concentration, high EPS-decay rate or slow EPS-production rate. Fig. 6 shows results obtained from the simulations, where the efficacy of a treatment is evaluated by the treatment time necessary for a tenfold decrease in biofilm active mass ($T_{10\%}$). As expected, efficacy of the treatment (characterized by a lower $T_{10\%}$) increases with increasing values of *Da* and decreasing values of ϕ. For cases where *Da* is low (production of EPS is much faster than decay due to DPA) and ϕ is high (degradation of DPA in biofilm is relatively fast compared with diffusion of DPA), the full removal of biofilm may not be accomplished, even for treatments with the DPA up to 100 h. In these conditions, DPA either decays too quickly or penetrates the biofilm too slowly and EPS either decays slowly or is produced quickly by the micro-organisms. Interestingly, for these cases, the model simulations predict the existence of persistent biofilm even in the presence of the DPA, with a

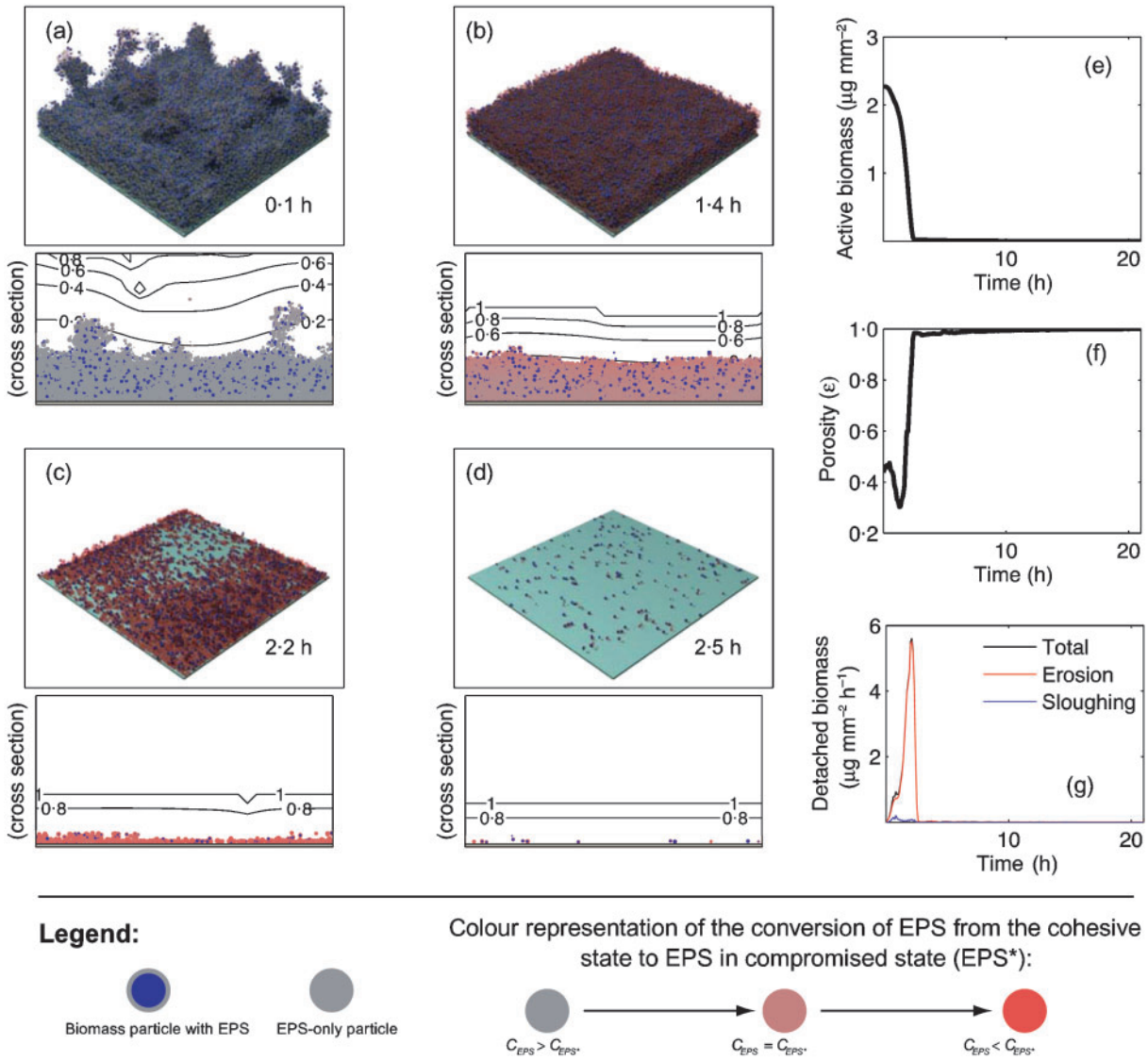

Fig. 5. Results for simulation of the action of a DPA on a 60-day-old biofilm. Simulations were carried out at $\phi = 3{\cdot}6$, $Da = 0{\cdot}71$ and $Y_{EPS^*} = 1$. (a–d) Biofilm structure after 0·1, 1·4, 2·2 and 2·5 h treatment with DPA. For each 3D structure, a 2D cross section through the biofilm is shown together with isoconcentration curves of DPA (normalized values). (e) Decrease in active biomass in the biofilm. (f) Change in biofilm porosity during the treatment. (g) Dynamics of biomass detachment (by erosion and sloughing) in the course of the treatment.

steady state in which detachment is balanced by biofilm growth.

Treatment with DPA – effect of Y_{EPS^*}

Values of Y_{EPS^*} of <1 represent cases where the EPS degradation to EPS* by DPA leads to a reduction of the total EPS mass in the matrix. Fig. 7(a) presents the time course of the reduction of active mass in the biofilm for a series of simulations with Y_{EPS^*} ranging from 1 to 0 ($\phi = 3{\cdot}6$, $Da = 0{\cdot}71$). The results show decreased treatment effectiveness with decreasing Y_{EPS^*}. Due to the practically complete decay of the EPS when $Y_{EPS^*} = 0$ and 0·01, the treatment with DPA produces a more dense and confluent biofilm, as EPS is assumed to be less dense than active mass. As detachment speed is inversely proportional to the local biofilm density in the expression used (equation 16), the formation of a biofilm with less EPS generates a structure less susceptible to erosion forces. Consequently, it is observed from the time course of active mass that, after an initial reduction in biomass, the biofilm starts to grow despite the presence of the DPA. This derives from the fact that using a low value for Y_{EPS^*} effectively represents cases where EPS does not play a significant role in the biofilm

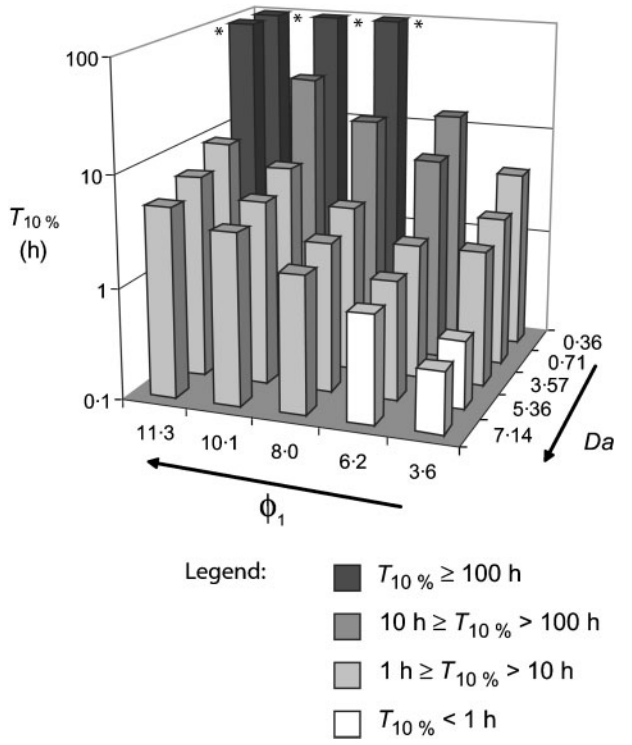

Fig. 6. Efficiency of biofilm removal with a DPA. The bar plot shows the treatment time necessary for a tenfold decrease in biofilm active mass ($T_{10\%}$) for simulations carried out at a range of values of ϕ and *Da*. Shading of the bars represents the range of the $T_{10\%}$ for each simulation, with lower $T_{10\%}$ values corresponding to a more efficient treatment. Asterisks shown next to a bar represent cases where a tenfold decrease in the biofilm active mass was not achieved up to the end of the simulation at 100 h treatment. Simulations were carried out with $Y_{EPS^*} = 1$ and $\gamma = 10$.

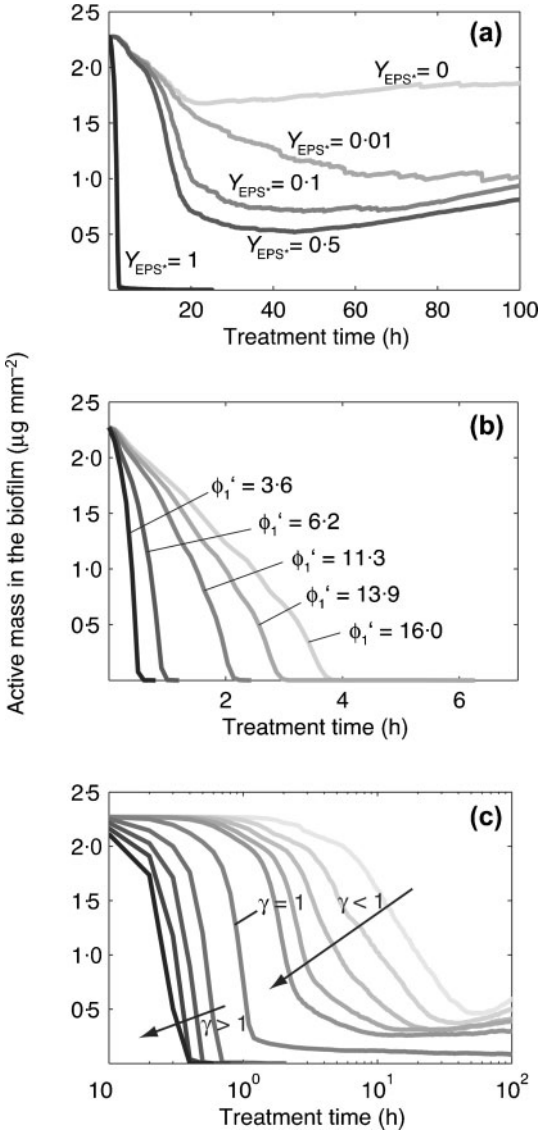

Fig. 7. (a) Time course of active mass in the biofilm in the presence of a DPA when the EPS matrix is decomposed in different degrees, simulated by four different Y_{EPS^*} values: 0, 0·01, 0·1, 0·5 and 1. Simulations were executed with $\phi = 3{\cdot}6$ and $Da = 0{\cdot}71$. (b) Time course of active mass in the biofilm for the case where the DPA is involved in a stoichiometric reaction with the EPS. Simulations were carried out with values for ϕ' of 3·6, 6·2, 11·3, 13·9 and 16·0, $Da = 0{\cdot}71$ and $Y_{EPS^*} = 1$. (c) Time course of active mass in the biofilm for simulations carried out at different orders of the dependence of the biofilm cohesiveness on f_{EPS}, γ from equations (15) and (16) (with $\phi = 3{\cdot}6$ and $Da = 0{\cdot}71$). Simulations were performed with $\gamma = 1$ (indicated in plot), five simulations with $\gamma < 1$ (indicated in plot, with arrow representing series carried out with increasing values of γ) and four simulations with $\gamma > 1$ (indicated in plot, with arrow representing series carried out with increasing values of γ).

cohesiveness, i.e. in binding the biofilm together. This issue is central for concluding that a biofilm with a low content of EPS may in fact develop, which may be the case in *Pseudomonas aeruginosa* biofilms. For such biofilms, experimental results suggest that alginate may not play a role in the cohesiveness of the biofilm matrix (Christensen *et al.*, 2001). Modelling the cases where the EPS plays a role in biofilm cohesiveness is represented by using higher values of Y_{EPS^*}.

DPA involved in a stoichiometric reaction with the EPS

The theoretical approach proposed here can be further adapted to represent the case in which the DPA is consumed as a result of its involvement in a stoichiometric reaction. This corresponds, for example, to the case in which the DPA is a chelating agent that sequesters multivalent cations from the EPS structure. In this case, there is no degradation of the EPS to soluble material. All of the EPS mass will remain in the biofilm and only its material properties will be affected (i.e. EPS is converted to EPS*). Also, the DPA is inactivated by reacting with the EPS. The decay of DPA is no longer

Table 5. Stoichiometry and rates of reactions adapted for the case where DPA is involved in a stoichiometric reaction with EPS

Process	Solute species		Particulate species			Rate
	Substrate (*S*)	DPA	Active biomass (*X*)	EPS – cohesive state (EPS)	EPS – compromised state (EPS*)	
Growth	$-Y_S$		1	Y_{EPS}		$\mu^{max}\frac{C_S}{C_S+K_S}C_X$
EPS decay		$-Y_{DPA}$		-1	1	$k_{EPS,dec}\frac{C_{EPS}}{C_{EPS}+K_{EPS}}C_{DPA}$

governed by equation (7). Instead, the following equation is used:

$$r_{DPA,dec} = Y_{DPA}k_{EPS,dec}\frac{C_{EPS}}{C_{EPS}+K_{EPS}}C_{DPA} \quad [M_{DPA}\ L^{-3}\ T^{-1}] \quad (19)$$

where Y_{DPA} is the yield of DPA consumed per decaying EPS. Table 5 contains the stoichiometry and reaction rates for the system adapted to account for DPA consumption in EPS degradation (cf. equation 19). For this case, the Thiele modulus for the DPA must be redefined as follows:

$$\phi'^2 = \frac{Y_{DPA}k_{EPS,dec}L_f^2}{D_{DPA}} \qquad [\text{dimensionless}] \qquad (20)$$

This new number, ϕ', groups the yield Y_{DPA} with $k_{EPS,dec}$ in a dimensionless group. Fig. 7(b) shows the time course of the decrease in active biomass in the biofilm for five simulations carried out at different values of ϕ'. These results show that, also for this case, the effectiveness of the treatment decreases with the increase in ϕ', thus with a less-diffusible DPA or with a slowly degradable EPS.

Effect of γ on biofilm removal

Parameter γ defines the order of the dependence of biofilm cohesiveness on the fraction f_{EPS} through equation (15). The effect of γ on the effectiveness of the DPA treatment was assessed by carrying out simulations with values of γ ranging from 0·2 to 10. Fig. 7(c) shows the time course of the decrease in active biomass in the biofilm obtained from those simulations (carried out with $\phi = 3{\cdot}6$ and $Da = 0{\cdot}71$). The results show that the predicted effectiveness of the biofilm treatment is highly dependent on the value of γ used. Simulations carried out with $\gamma > 1$ predicted full biofilm removal within 100 h simulated treatment with a DPA. At $\gamma \leqslant 1$, meaning a weaker dependency of biofilm cohesiveness on the EPS fraction, the simulations did not predict full removal within 100 h. Furthermore, all simulations performed with values of γ lower than 1 predicted a subsequent boost in biofilm development after an initial decrease in biofilm active mass. Presently, there are no experimental data available on the literature that could be used to determine γ. Possible experimental methods to measure γ are proposed in the Discussion.

DISCUSSION

Model-based simulations of biofilm removal by treatment with a DPA provide a quantitative framework for evaluating the importance of mass-transport characteristics of the DPA and its reaction with biofilm EPS. The Thiele moduli ϕ and ϕ' quantify the relationship between DPA decay rate and its diffusion into the biofilm structure. The decay of EPS by reacting with a DPA, quantified by the Damköhler number (*Da*), is also highly important in defining the efficacy of a treatment. Simulations carried out at diverse values of ϕ and *Da* suggest that efficacy of a treatment decreases with decreasing ϕ and increasing *Da* (Fig. 6). That is, as one would logically expect, if the DPA decays too quickly or it diffuses across the biofilm too slowly, if the EPS decays slowly or if it is produced too quickly, then diminished biofilm removal is achieved. In those conditions, a thick biofilm with a high EPS content may persist in spite of the presence of a DPA.

The dual-state representation for EPS proposed here and the parameter Y_{EPS^*} allow the description of several DPA action scenarios. Such scenarios range from cases where EPS mass is converted entirely to a non-cohesive substance, the compromised state, to cases where the EPS does not play a role in the biofilm cohesiveness. The latter case, represented by setting $Y_{EPS^*} = 0$, assumes that no conversion to a compromised state exists. Intermediate scenarios, where the solid EPS matrix is partially converted to EPS* ('compromised' EPS) and partially dissolved, are simulated by using values of Y_{EPS^*} between 0 and 1. The simulations carried out at a range of Y_{EPS^*} values (Fig. 7a) indicate that DPAs whose action is directed at affecting the biofilm cohesiveness (represented by values of Y_{EPS^*} closer to 1) may be the most effective in removing the biofilm. DPAs whose action is directed at degrading EPSs that do not influence the biofilm cohesiveness (cases represented by using low Y_{EPS^*} values) may not be a suitable strategy for removing the biofilm. Results from simulations for these cases predict that biofilms that are thin and dense and that have a high content of active microbial biomass will result from the treatment, rather than full removal of the biofilm. This prediction is purely theoretical and only valid if the assumptions presented in the model formulation are themselves valid. Nevertheless, the mechanism observed here may be a possible explanation

for the experimentally observed failure of alginate lyase to remove *P. aeruginosa* biofilms when the same enzyme is able to degrade alginate in other settings (Christensen *et al.*, 2001).

The parameter γ, used here to define the order of the dependence of the biofilm cohesiveness on the fraction f_{EPS}, was also observed to be highly important for the efficacy of a treatment scenario. This was revealed from the results shown in Fig. 7(c). The value of γ represents the importance that the EPS component affected by the DPA has on the biofilm cohesiveness. $\gamma=1$ indicates that biofilm cohesiveness is affected linearly as EPS is converted to EPS*. Values of $\gamma>1$ may represent, for example, cases where the component affected by DPA is involved in several structural bonds in the EPS matrix. In such cases, biofilm cohesiveness could be affected non-linearly and with an order of f_{EPS} higher than 1. Values of $\gamma<1$ represent, in turn, the opposite scenario, where the affected EPS component does not play an important role in defining the EPS cohesiveness. Experimental values for parameters such as γ are presently unavailable, although experimental techniques exist that may potentially be applied to obtain such information. The method proposed by Ohashi & Harada is based on applying both tensile force and shear force and was used successfully to measure adhesion strength of denitrifying biofilms (Ohashi & Harada, 1996) and biofilms grown under different conditions (Ohashi *et al.*, 1999). A method developed recently that uses micro-cantilevers (Poppele & Hozalski, 2003) to measure the tensile strength of biofilms and microbial flocs could be used to determine the alteration in biofilm strength as a consequence of the presence of a DPA substance. Results from such experiments would allow derivation of a function for the alteration of the biofilm cohesive strength.

The study presented here comprises four simulations of undisturbed biofilm growth and 43 simulations of biofilm-treatment scenarios. Animated visualizations of biofilm-structure evolution during the treatment with DPA may be obtained for all simulations from our website at http://www.biofilms.bt.tudelft.nl/biofilmControl/index.html.

Of all of the simulations of biofilm treatment, however, only a limited number predicted a successful, complete biofilm removal. A common pattern was observed in all of the simulations predicting complete biofilm removal: an initial rapid removal of the largest part of the biofilm occurs within the first moments after introduction of the DPA in the medium. Following this initial period, removal of the remaining portion of the biofilm requires a relatively long period, still in the presence of the DPA. This last portion of the biofilm often consists of a thin and sparse layer of biofilm. The simulation results shown in Fig. 5 exemplify this observation, as analysed previously in the Results. From an analysis of these simulation results, we can conclude that the persistence of a last sparse layer of biomass results (i) from a lower detachment rate acting on thinner biofilms (because the detachment-speed function decreases as the biofilm thickness decreases) and (ii) from higher specific-growth and EPS-production rates for the thin biofilm (because of lower mass-transfer limitations and lower amounts of biomass sharing the substrate). The removal of the last fraction of the biofilm may constitute the majority of the time required for full biofilm removal, as was the case for the simulation shown in Fig. 5. For this simulation, as stated earlier, detachment of the last 1 % of the micro-organisms required 94 % of the total treatment time. This fact alerts to the necessity of a more precise knowledge of the detachment dynamics of the bacteria attached directly to the solid substratum for an accurate prediction of the efficiency of treatment using modelling techniques.

Other parameters related to the action of a DPA, i.e. reaction-rate coefficients, reaction yields and diffusivity coefficients, are also presently unavailable in the literature. Due to the absence of extensive information on the mechanisms of action of DPAs, the model presented here was kept as simple and generic as possible, but was still based on widely accepted principles. The framework used to construct the model allows even more detailed representations of the biomass. Biofilm models defined in this framework may include inert formation and multiple microbial species, as shown in previous studies (Xavier *et al.*, 2005a, b). Introducing more detail into the biomass description here would have been undesirable, as it would create the necessity for more assumptions and complicate derivation of the trends reported. However, if more information is made available in the future from experimental characterization of biofilm-removal experiments, the model can easily be extended to accommodate new processes or biomass components. For example, it is expected that, for older biofilms, the formation of inert material will play a role in biofilm cohesiveness, as inert material will not grow or produce more EPS and its presence may affect the biofilm cohesiveness.

Conclusions

The modelling approach proposed here, consisting of a theoretical framework and its numeric implementation by using IbM, allowed the prediction of the efficacy of biofilm-control scenarios by using DPAs. The results of simulations carried out by using several sets of parameters produced the following conclusions.

The efficacy of using a DPA for removing a biofilm will be highly dependent on: (i) the balance between the mass-transport properties of the DPA through the biofilm matrix and its decay rate (quantified by Thiele moduli); (ii) the balance between the kinetics of action of the DPA on the EPS and EPS production by the micro-organisms [which may be quantified by the Damköhler number proposed in equation (18)]; and (iii) the mechanisms of influence of the DPA on the EPS, included in the model through the parameters Y_{EPS^*} and γ.

For cases where treatment with a DPA does result in complete removal of the biofilm, it is expected that the removal

will follow a pattern where the majority of the biofilm biomass is removed in the initial instants of the treatment, but the removal of the last fraction of the biofilm will take a considerably larger fraction of the total treatment time.

The results from simulations presented here alert for the necessity to investigate experimentally the effect of DPAs on biofilm cohesiveness. This is essential for the accurate prediction of the efficiency of control strategies using modelling approaches.

REFERENCES

Abdul Rani, S., Pitts, B. & Stewart, P. S. (2005). Rapid diffusion of fluorescent tracers into *Staphylococcus epidermidis* biofilms visualized by time lapse microscopy. *Antimicrob Agents Chemother* **49**, 728–732.

Allison, D. G., Ruiz, B., SanJose, C., Jaspe, A. & Gilbert, P. (1998). Extracellular products as mediators of the formation and detachment of *Pseudomonas fluorescens* biofilms. *FEMS Microbiol Lett* **167**, 179–184.

Boyd, A. & Chakrabarty, A. M. (1994). Role of alginate lyase in cell detachment of *Pseudomonas aeruginosa*. *Appl Environ Microbiol* **60**, 2355–2359.

Boyd, A. & Chakrabarty, A. M. (1995). *Pseudomonas aeruginosa* biofilms: role of the alginate exopolysaccharide. *J Ind Microbiol Biotechnol* **15**, 162–168.

Chen, X. & Stewart, P. S. (2000). Biofilm removal caused by chemical treatments. *Water Res* **34**, 4229–4233.

Chen, X. & Stewart, P. S. (2002). Role of electrostatic interactions in cohesion of bacterial biofilms. *Appl Microbiol Biotechnol* **59**, 718–720.

Christensen, B. E., Ertesvag, H., Beyenal, H. & Lewandowski, Z. (2001). Resistance of biofilms containing alginate-producing bacteria to disintegration by an alginate degrading enzyme (AlgL). *Biofouling* **17**, 203–210.

Cui, W., Winter, W. T., Tanenbaum, S. W. & Nakas, J. P. (1999). Purification and characterization of an intracellular carboxylesterase from *Arthrobacter viscosus* NRRL B-1973: physical and spectroscopic characterization and evaluation as models for cellulose triacetate. *Enzyme Microb Technol* **24**, 200–208.

Gordon, C. A., Hodges, N. A. & Marriott, C. (1991). Use of slime dispersants to promote antibiotic penetration through the extracellular polysaccharide of mucoid *Pseudomonas aeruginosa*. *Antimicrob Agents Chemother* **35**, 1258–1260.

Grotenhuis, J. T. C., van Lier, J. B., Plugge, C. M., Stams, A. J. M. & Zehnder, A. J. B. (1991). Effect of ethylene glycol-bis(*β*-aminoethyl ether)-*N*,*N*-tetraacetic acid (EGTA) on stability and activity of methanogenic granular sludge. *Appl Microbiol Biotechnol* **36**, 109–114.

Hermanowicz, S. W. (2001). A simple 2D biofilm model yields a variety of morphological features. *Math Biosci* **169**, 1–14.

Higgins, M. J. & Novak, J. T. (1997). The effect of cations on the settling and dewatering of activated sludges: laboratory results. *Water Environ Res* **69**, 215–224.

Horn, H., Neu, T. R. & Wulkow, M. (2001). Modelling the structure and function of extracellular polymeric substances in biofilms with new numerical techniques. *Water Sci Technol* **43**, 121–127.

Huebner, J. & Goldmann, D. A. (1999). Coagulase-negative staphylococci: role as pathogens. *Annu Rev Med* **50**, 223–236.

Hughes, K. A., Sutherland, I. W. & Jones, M. V. (1998). Biofilm susceptibility to bacteriophage attack: the role of phage-borne polysaccharide depolymerase. *Microbiology* **144**, 3039–3047.

Hunt, S. M., Hamilton, M. A., Sears, J. T., Harkin, G. & Reno, J. (2003). A computer investigation of chemically mediated detachment in bacterial biofilms. *Microbiology* **149**, 1155–1163.

Hunt, S. M., Werner, E. M., Huang, B., Hamilton, M. A. & Stewart, P. S. (2004). Hypothesis for the role of nutrient starvation in biofilm detachment. *Appl Environ Microbiol* **70**, 7418–7425.

Itoh, Y., Wang, X., Hinnebusch, B. J., Preston, J. F., III & Romeo, T. (2005). Depolymerization of *β*-1,6-*N*-acetyl-D-glucosamine disrupts the integrity of diverse bacterial biofilms. *J Bacteriol* **187**, 382–387.

Jass, J. & Walker, J. T. (2000). Biofilms and biofouling. In *Industrial Biofouling: Detection, Prevention and Control*, pp. 1–12. Edited by J. T. Walker, S. Surman & J. Jass. New York: Wiley.

Johansen, C., Falholt, P. & Gram, L. (1997). Enzymatic removal and disinfection of bacterial biofilms. *Appl Environ Microbiol* **63**, 3724–3728.

Kaplan, J. B., Ragunath, C., Ramasubbu, N. & Fine, D. H. (2003). Detachment of *Actinobacillus actinomycetemcomitans* biofilm cells by an endogenous *β*-hexosaminidase activity. *J Bacteriol* **185**, 4693–4698.

Kaplan, J. B., Ragunath, C., Velliyagounder, K., Fine, D. H. & Ramasubbu, N. (2004). Enzymatic detachment of *Staphylococcus epidermidis* biofilms. *Antimicrob Agents Chemother* **48**, 2633–2636.

Kreft, J.-U. & Wimpenny, J. W. T. (2001). Effect of EPS on biofilm structure and function as revealed by an individual-based model of biofilm growth. *Water Sci Technol* **43**, 135–141.

Lewandowski, Z., Beyenal, H. & Stookey, D. (2004). Reproducibility of biofilm processes and the meaning of steady state in biofilm reactors. *Water Sci Technol* **49**, 359–364.

Mayer, C., Moritz, R., Kirschner, C., Borchard, W., Maibaum, R., Wingender, J. & Flemming, H.-C. (1999). The role of intermolecular interactions: studies on model systems for bacterial biofilms. *Int J Biol Macromol* **26**, 3–16.

Nielsen, P. H., Frølund, B. & Keiding, K. (1996). Changes in the composition of extracellular polymeric substances in activated sludge during anaerobic storage. *Appl Microbiol Biotechnol* **44**, 823–830.

Ohashi, A. & Harada, H. (1996). A novel concept for evaluation of biofilm adhesion strength by applying tensile force and shear force. *Water Sci Technol* **34**, 201–211.

Ohashi, A., Koyama, T., Syutsubo, K. & Harada, H. (1999). A novel method for evaluation of biofilm tensile strength resisting erosion. *Water Sci Technol* **39**, 261–268.

Picioreanu, C., van Loosdrecht, M. C. M. & Heijnen, J. J. (2001). Two-dimensional model of biofilm detachment caused by internal stress from liquid flow. *Biotechnol Bioeng* **72**, 205–218.

Picioreanu, C., Kreft, J.-U. & van Loosdrecht, M. C. M. (2004). Particle-based multidimensional multispecies biofilm model. *Appl Environ Microbiol* **70**, 3024–3040.

Pizarro, G., Griffeath, D. & Noguera, D. R. (2001). Quantitative cellular automaton model for biofilms. *J Environ Eng* **127**, 782–789.

Poppele, E. H. & Hozalski, R. M. (2003). Micro-cantilever method for measuring the tensile strength of biofilms and microbial flocs. *J Microbiol Methods* **55**, 607–615.

Rittmann, B. E., Schwarz, A. O., Eberl, H. J., Morgenroth, E., Perez, J., van Loosdrecht, M. & Wanner, O. (2004). Results from the multispecies Benchmark Problem (BM3) using one-dimensional models. *Water Sci Technol* **49**, 163–168.

Skillman, L. C., Sutherland, I. W. & Jones, M. V. (1999). The role of exopolysaccharides in dual species biofilm development. *J Appl Microbiol* **85** (Suppl. 1), 13S–18S.

Staudt, C., Horn, H., Hempel, D. C. & Neu, T. R. (2004). Volumetric measurements of bacterial cells and extracellular polymeric substance glycoconjugates in biofilms. *Biotechnol Bioeng* **88**, 585–592.

Stewart, P. S. (1993). A model of biofilm detachment. *Biotechnol Bioeng* **41**, 111–117.

Stewart, P. S., McFeters, G. A. & Huang, C. T. (2000). Biofilm control by antimicrobial agents. In *Biofilms II: Process Analysis and Applications*, pp. 373–405. Edited by J. D. Bryers. New York: Wiley.

Sutherland, I. W. (2001). Biofilm exopolysaccharides: a strong and sticky framework. *Microbiology* **147**, 3–9.

Thormann, K. M., Saville, R. M., Shukla, S. & Spormann, A. M. (2005). Induction of rapid detachment in *Shewanella oneidensis* MR-1 biofilms. *J Bacteriol* **187**, 1014–1021.

Tsuneda, S., Aikawa, H., Hayashi, H., Yuasa, A. & Hirata, A. (2003). Extracellular polymeric substances responsible for bacterial adhesion onto solid surface. *FEMS Microbiol Lett* **223**, 287–292.

Turakhia, M. H., Cooksey, K. E. & Characklis, W. G. (1983). Influence of a calcium-specific chelant on biofilm removal. *Appl Environ Microbiol* **46**, 1236–1238.

van Casteren, W. H. M., Dijkema, C., Schols, H. A., Beldman, G. & Voragen, A. G. J. (1998). Characterisation and modification of the exopolysaccharide produced by *Lactococcus lactis* subsp. *cremoris* B40. *Carbohydr Polymers* **37**, 123–130.

Wanner, O. & Gujer, W. (1986). A multispecies biofilm model. *Biotechnol Bioeng* **28**, 314–328.

Whitchurch, C. B., Tolker-Nielsen, T., Ragas, P. C. & Mattick, J. S. (2002). Extracellular DNA required for bacterial biofilm formation. *Science* **295**, 1487.

Wingender, J., Neu, T. R. & Flemming, H.-C. (1999). What are bacterial extracellular polymeric substances? In *Microbial Extracellular Polymeric Substances: Characterization, Structure and Function*, pp. 1–20. Edited by J. Wingender, T. R. Neu & H.-C. Flemming. New York: Springer.

Xavier, J. B., Picioreanu, C. & van Loosdrecht, M. C. M. (2004). A modelling study of the activity and structure of biofilms in biological reactors. *Biofilms* **1**, 377–391.

Xavier, J. B., Picioreanu, C. & van Loosdrecht, M. C. M. (2005a). A framework for multidimensional modelling of activity and structure of multispecies biofilms. *Environ Microbiol* **7**, 1085–1103.

Xavier, J. B., Picioreanu, C. & van Loosdrecht, M. C. M. (2005b). A general description of detachment for multidimensional modelling of biofilms. *Biotechnol Bioeng* **91**, 651–669.

Xun, L., Mah, R. A. & Boone, D. R. (1990). Isolation and characterization of disaggregatase from *Methanosarcina mazei* LYC. *Appl Environ Microbiol* **56**, 3693–3698.